Proceedings of the Estonian Academy of Sciences
2025, **74**, 2S, 322–331

https://doi.org/10.3176/proc.2025.2S.07

www.eap.ee/proceedings
Estonian Academy Publishers

DIGITAL SIGNAL PROCESSING

RESEARCH ARTICLE

Received 20 December 2024
Accepted 2 April 2025
Available online 17 June 2025

Keywords:
mobile networks, localization, UAVs, 5G

Corresponding author:
Alberto Facheris
alberto.facheris@polimi.it

Citation:
Reggiani, L. and Facheris, A. 2025. Impact of multipath on anchor selection strategies for UAV localization in mobile networks. *Proceedings of the Estonian Academy of Sciences*, **74**(2S), 322–331. https://doi.org/10.3176/proc.2025.2S.07

Impact of multipath on anchor selection strategies for UAV localization in mobile networks

Luca Reggiani and Alberto Facheris

Technical University of Milan, Piazza Leonardo da Vinci 32, 20133 Milan, Italy

ABSTRACT

Positioning is gaining increasing importance in mobile systems due to its potential integration with many 5G verticals. In non-terrestrial networks, positioning of aerial vehicles constitutes a crucial element of the communication, control, and applications of these systems. Unmanned aerial vehicles (UAVs) have become strategic actors in this technical and economic trend. A distinctive feature of UAV positioning in mobile networks is that signals from multiple base stations, or anchors, can typically be received and employed for localization, as propagation conditions, including the fundamental line of sight availability, improve with altitude. However, this advantage poses serious issues in terms of computational complexity, channel occupation, and latency unless an appropriate selection of available anchors is performed. In this work, we investigate and discuss several anchor selection strategies under realistic propagation scenarios, with an emphasis on the impact of multipath, according to the 3GPP channel models for aerial vehicles. The application of these strategies to channels affected by multipath using a standard least squares positioning technique reveals interesting properties and design directions for a feasible solution to the anchor selection problem. Notably, we show that even 3 or 4 well-selected anchors are often sufficient to achieve sub-meter 3D positioning accuracy.

1. Introduction

In modern 5G systems and applications, localization is gaining increasing interest, as it provides fundamental advantages in several scenarios, including industrial ones. Starting from Release 16 (3GPP 2018a) of the 5G specifications, we have seen growing attention toward positioning techniques in different deployment scenarios and use cases. Standard techniques based on cell identity (Cell-ID), round-trip-time (RTT), angle of arrival (AoA), angle of departure (AoD), and time difference of arrival (TDoA) constitute the core of the new radio (NR) positioning system and are configured in either uplink or downlink through the introduction of novel dedicated signals and procedures. In particular, the introduction of positioning reference signals (PRSs), which enable accurate estimation of time-of-arrival (ToA) and support RTT capabilities, is of great importance for 3D localization. This is especially relevant in the context of unmanned aerial vehicles (UAVs), which can benefit from improved aerial traffic management, enhanced positioning accuracy, and better integration with other non-terrestrial devices and systems, such as aircrafts, high-altitude aerial platforms, and satellites.

The implementation of highly precise horizontal and vertical positioning functions has been addressed since Release 17 (3GPP 2022), which also introduced several enhancements, ranging from improved network efficiency (e.g., on-demand transmission of PRSs) to better device efficiency, reduced latency, and support for high integrity and reliability requirements in positioning (3GPP 2023a). Further improvements are expected with the upcoming Release 18 (3GPP 2023b), which aims to enable ultra-high positioning accuracy – down to centimeter-level – for industrial internet of things (IIoT) use cases, through the introduction of carrier phase positioning, reduced capability user equipment (UE) with positioning support, and sidelink positioning.

High-altitude aerial platforms, aircraft communication, and UAVs have been the subject of considerable interest in the 3GPP standardization process since the deployment of 4G. It is needless to list all the applications of UAVs – from logistics to agriculture and emergency communications – and the related need for resilient and powerful connectivity and positioning systems for their control and for advanced air traffic management systems. Since Release 15 (3GPP 2018b), increasing efforts have been devoted to understanding the performance of mobile networks when used to serve aerial vehicles, as well as to defining the directions and solutions for enhancing their integration and connectivity (3GPP 2017). More recently, during the development of Release 17 (3GPP 2022), a wide range of applications and scenarios for low-altitude UAVs was considered, such as high-resolution video live broadcast, autonomous flight, aerial communications, and others (3GPP 2019). In addition, full support for advanced unmanned aerial systems connectivity, identification, and tracking in the context of 3GPP systems and unmanned aircraft system traffic management (UTM) authorities is becoming a crucial requirement (3GPP 2021).

In the context of anchor selection and network planning, previous works have mainly focused on the maximization of data rate, coverage extension, and the reliability and integrity of communications. Few studies have approached the problem of anchor selection for a 3D localization-oriented use case within 5G networks, and none exist for the specific application of UAVs. In Xhafa et al. (2022), a 5G-based localization method is studied that jointly exploits uplink TDoA and AoA, aided by a base station (BS) exclusion method capable of detecting and eliminating measurements affected by non-line-of-sight (NLoS) conditions. In Deng et al. (2020), through the analysis of the geometric dilution of precision, it is shown that a BS selection strategy based only on channel conditions is not fully satisfactory for hybrid positioning, where the estimate is achieved by the concurrent use of TDoA, RTT, and direction-of-arrival (DoA) measurements combined with a prior position estimate to be updated. In Albaidhani et al. (2019), indoor localization using a limited number of ultra-wideband (UWB) nodes is studied, and an algorithm for optimal anchor selection is proposed, feasible for scenarios with a low number of available anchors.

This work builds on the study presented in Facheris and Reggiani (2023), in which we derived a mathematical framework to evaluate the localization accuracy bound achievable in the context of 5G networks and, based on this formulation, proposed several anchor selection strategies. The selection is performed according to the strategies described in Section 4. This paper is an extended version of Reggiani and Facheris (2024), and the main contributions are the following:

1. Evaluation of the impact of multipath on ranging and positioning precision in the 3D case of UAVs.
2. Simulation and discussion of strategies for decreasing the number of anchors (when redundant), in the presence of multipath and NLoS.
3. Analysis of the impact of applying a real localization algorithm, i.e., nonlinear least squares (NLLS), on the performance and selection of anchors.
4. The inclusion of multipath and a real algorithm reveal cases where a simple signal-to-noise-ratio (SNR)-based selection technique is a satisfactory solution to a potentially complex problem. At the same time, the most sophisticated solution, denoted as "*J*-iterative," consistently preserves the best performance when reducing the number of anchors.
5. Compared to Reggiani and Facheris (2024), this paper presents additional and more exhaustive numerical results, enabling a more detailed and structured evaluation of the potential of the techniques exploited for reducing the number of anchors.

The paper is structured as follows. Section 2 presents the system and signal models considered for the study, while Sections 3 and 4 describe the algorithms used to evaluate the positioning bound and the performance of practical algorithms. Section 4 also introduces the anchor selection approaches, and Section 5 presents and discusses the numerical results and comparisons.

2. System model

Our scenario consists of an area (2000 × 2000 m) in which a UAV has to be located through 5G signals emitted or received by a set of BSs or anchors. The anchors are perfectly synchronized with each other, and their exact positions are known. The scenario is composed of a rectangular grid of 25 BSs equipped with omni-directional antennas, which are suited to model a 5G/5G-Advanced network capable of emitting beams in all directions with similar power intensities. In Fig. 1b, the grid of points at which the positioning performance is evaluated is shown: with respect to Reggiani and Facheris (2024), in which only the positions marked by black points were simulated, here the denser grid of gray points has been added to refine the numerical results. Between each anchor and the UAV, the 3D direction is given by the relative azimuth and elevation angles, as depicted in Fig. 2. Further details of the system model are listed below:

- The anchors are placed 500 m apart from each other, and each anchor is located at an altitude of 25 m.
- Only an isotropic beam is emitted by each BS. Please note that this scenario is equivalent to a set of beams, emitted by large antenna arrays, that potentially cover all directions in space.
- The system operates at a carrier frequency of 3.6 GHz, transmitting the PRSs according to a muting pattern scheme to prevent mutual interference (3GPP 2023c). The PRSs span 12 symbols and 52 resource blocks, with a subcarrier spacing of 15 kHz and a total bandwidth of $B = 10$ MHz.
- The equivalent isotropic radiated power (EIRP) is set to 3.16 W (35 dBm), and the power spectral density of the noise to $N_0 = 2 \times 10^{-20}$ J.
- The UAV is placed inside a square grid of points at different altitudes, from 30 to 300 m. As shown in Fig. 1b, a grid with higher point density at the center of the scenario is simulated to derive more accurate results and a more detailed distribution of the errors.
- Phase noise, Doppler effect, and other impairments are neglected.
- The channel is modeled according to 3GPP (2017). Therefore, the numerical results take into account the impact of path loss, shadowing, multipath, and line-of-sight (LoS) conditions as a function of altitude (between 30 and 300 m). The environment selected for this study is the urban macro (UMa) scenario defined in 3GPP (2017),

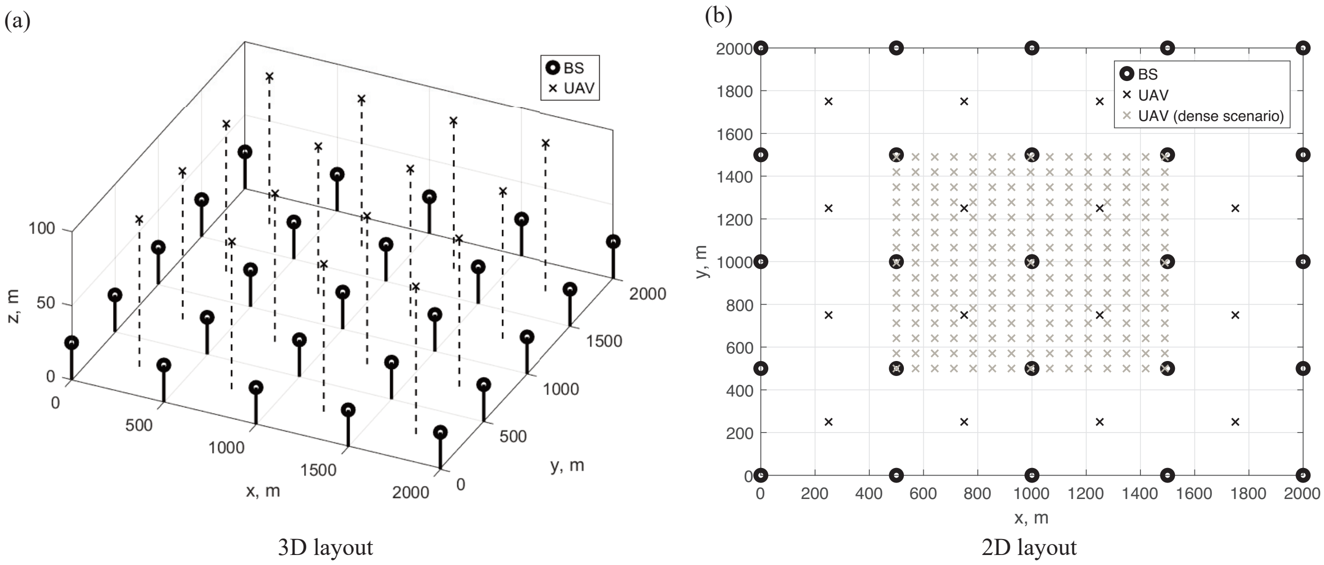

Fig. 1. Geometric layout (2D and 3D) of the base stations (BS) and unmanned aerial vehicle (UAV) positions used in the simulations.

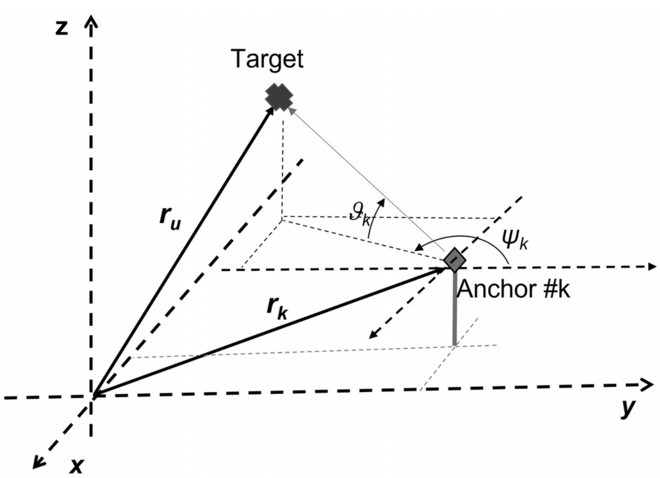

Fig. 2. Relative angles, elevation and azimuth (υ_k, ψ_k), between the target and the k-th anchor.

which is the most challenging and interesting in terms of the expected applications.

- The SNR is defined, for the generic j-th link, as

$$SNR_j = \frac{|\alpha_{j0}|^2 \cdot EIRP}{B \cdot N_0},$$

where α_{j0} is the first path complex channel gain of the j-th link.

3. Positioning performance bound

To achieve a lower bound on positioning performance, denoted as the squared positioning error bound (SPEB), we exploit the Cramér–Rao lower bound (CRLB) for the UAV position developed in Facheris and Reggiani (2023). This work includes the impact of multipath on each link under LoS or NLoS conditions, based on the SNR reduction model presented in Section 3.1. This measure represents the lowest possible mean squared error of an unbiased estimator, considering both the channel conditions and the geometric layout of the anchors.

Furthermore, we assume no a priori information about the UE position, and that the receiver clock is perfectly stable during the time interval required to receive all the signals employed to estimate the position. Two common cases are considered: timing synchronization between the UAV and the BSs, and absence of timing synchronization. The latter case is modeled by introducing an additional unknown timing offset (TO) in the estimation process.

The ranging error is modeled taking into account the multipath impact, as explained in Section 3.1. In addition, an outage probability is defined on the SPEB, as reported in Section 3.2. Finally, in some selected figures, the SPEB is presented in its vertical and horizontal components, denoted as $SPEB_V$ and $SPEB_H$, respectively, to highlight some interesting performance differences as a function of the UAV altitude.

3.1. Ranging error

The relation between the SNR and the ToA accuracy bound of the single link depends on the propagation conditions between the target and the anchor. There is a vast literature about the ToA accuracy bounds, developed particularly for wideband systems, where multipath has a significant impact. Excluding the performance regions at low SNRs, it is commonly assumed that the bias effect due to multipath becomes negligible and ToA errors are well described by the CRLB, which is inversely proportional to the SNR associated to the first LoS path. Following the derivation in Facheris and Reggiani (2023), the Time of Arrival CRLB for the j-th link is given as follows:

$$CRLB(\tau_j) = \frac{1}{16\pi^2 B \cdot T_{obs} \cdot \beta^2 \cdot (1-\chi) \cdot SNR_j}, \quad (1)$$

where T_{obs} is the duration of the PRS, β and B are the corresponding effective and actual signal bandwidths, and χ is a multipath factor introduced here to include the path-overlap phenomenon (Shen and Win 2010) (with $\chi = 0$ in free space or for $B \to \infty$). The effective bandwidth is given as follows:

$$\beta = \frac{\int |S_j(f)|^2 \, df}{\int f^2 |S_j(f)|^2 \, df}, \tag{2}$$

where $S_j(f)$ denotes the Fourier transform of $s_j(t)$. Exploiting the CRLB 3D ranging bound presented in Wang et al. (2017), we have evaluated the SNR reduction term $(1 - \chi)$ in Eq. (1) by simulating 500 UMa multipath realizations at different altitudes. We found that this term can be well approximated by a Gaussian variable in the dB domain, with mean and standard deviation equal to (–23.4, 3.7) dB for the LoS case and (–24.3, 8.2) dB for the NLoS case.

3.2. Positioning outage

To control the presence of outliers in the computation of the SPEB, averaged with respect to many positions and channel realizations, we define an outage in the positioning estimate if the error exceeds a threshold that depends on the altitude h, and precisely equal to $h/\sqrt{2}$. As the altitude increases, the distances from the BSs increase, along with the corresponding volume around the UAV of estimates considered acceptable in a realistic system. Therefore, in addition to the squared mean error, computed within the set of errors that are within the threshold, we report the probability that the error exceeds the threshold as the outage probability P_{OUT}.

4. Positioning techniques and anchor selection strategies

To estimate the position of the UAV and test the anchor selection strategies in a real positioning system, we have adopted the well-known NLLS algorithm (Bar-Shalom et al. 2002), defined as:

$$\hat{\mathrm{x}} = \arg\min_{\mathrm{x}} \sum_{k=1}^{N_A} \left(|\mathrm{x} - \mathrm{x}_k| - \rho_k \right)^2, \tag{3}$$

where x denotes the 3D position of the target, x_k denotes the 3D position of the k-th anchor, and ρ_k denotes the corresponding pseudorange. The implementation of the NLLS algorithm is carried out exploiting the nonlinear least-squares solver function of MATLAB *lsqnonlin()*, with default parameters. In particular, the maximum number of iterations is 400, and the termination tolerance on the first-order optimality is 10^{-6}.

The input of the algorithm is constituted by a set of distances with Gaussian errors, generated according to the CRLB in Eq. (1). In the case of NLoS links, which are discarded in the SPEB (Section 3), the distance error is also affected by a bias, computed assuming that the propagation path between the anchor and UAV has an angle of departure uniformly distributed between 45° and 80° relative to the LoS path, with just a single reflection. The resulting performance of the NLLS algorithm is measured by the mean squared positioning error (SPE) of the simulated positions estimates, i.e.,

$$SPE = \frac{1}{N} \sum_{n=1}^{N} \left(\mathrm{x}_n - \hat{\mathrm{x}}_n \right)^2, \tag{4}$$

where N is the number of simulations, x_n is the actual position of the target in the n-th simulation, and $\hat{\mathrm{x}}_n$ is the estimated position. The SPE is computed excluding errors that exceed the threshold defined in Section 3.2. These errors, treated as outliers in the estimation procedure, determine the outage probability P_{OUT}.

The problem of the selection strategies is approached by starting from the full set of available anchors, which can be potentially large for UAVs because of their altitude (simulations show that the signals from tens of BSs are detectable in terms of SNR), and recursively selecting the anchor to be excluded from the list. At each recursion, one anchor is removed and the process continues until the minimum number of anchors required for 3D position estimation is reached – either using ToA (assuming synchronization) or difference ToA (in the case of no synchronization between the UAV and the BSs). The strategies, adapted and refined from Facheris and Reggiani (2023), are briefly summarized in the following list.

1. **SNR**: This is the simplest strategy, in which the anchor with the worst SNR is discarded at each recursion.
2. **Distance**: The anchor farthest from the UAV is discarded at each recursion.
3. **Azimuth**: At each recursion, all azimuthal angles between the UAV and anchors (Fig. 2) are sorted into a vector, and the differences between consecutive angles are computed. The two anchors with the minimum azimuth difference are selected, and the one with the worst SNR is discarded. The principle is to discard the anchor with minimum impact on the azimuthal plane, as another anchor at the same angle is already present.
4. **Azimuth + elevation**: This strategy follows the same principle as the azimuth-based technique but also includes elevation to exclude the anchor that has a 3D path direction to the target UAV already covered by another one with better SNR.
5. ***J*-iterative**: This technique is based on the Fisher information matrix J derived for the computation of the bound. At each recursion, the impact of removing each anchor on the bound is evaluated by eliminating the corresponding columns in the matrices used to compute the bound. The anchor with the minimum SPEB reduction is discarded. This strategy, which is expected to yield the best results, is also the most computationally demanding. All parameters necessary for evaluating the SPEB (distances, angles, and link SNRs) are required. Except for the SNR-based strategy, which is the simplest, all other approaches require a priori knowledge of geometric parameters (distances and angles from anchors to the UAV), which could be estimated during a tracking process, exploiting the predicted position from the previous tracking step. In this paper, these parameters are assumed to be known perfectly.

5. Numerical results

Here we present the results, in terms of SPEB or SPE (NLLS algorithm), obtained from the scenarios presented in Section 2,

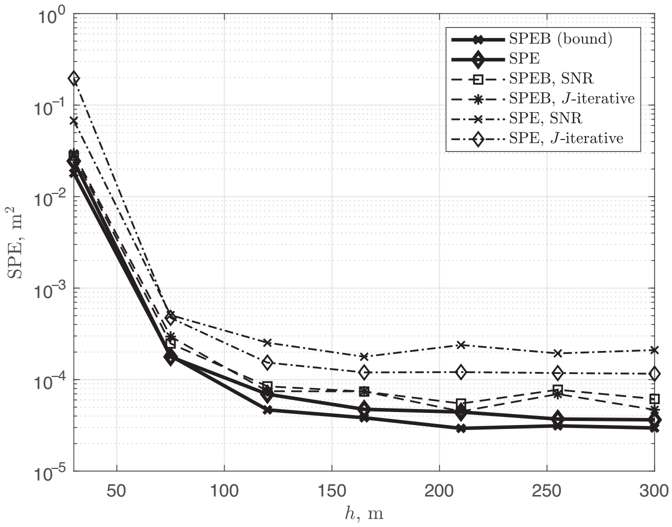

Fig. 3. SPEB (bound) and SPE (NLLS algorithm) using the SNR and J-iterative strategies, as a function of altitude h. The SPEB (bound) and SPE are computed with the maximum number of anchors, while the results for the other strategies are obtained with the maximum anchor reduction $N_{R,MAX}$ = 21.

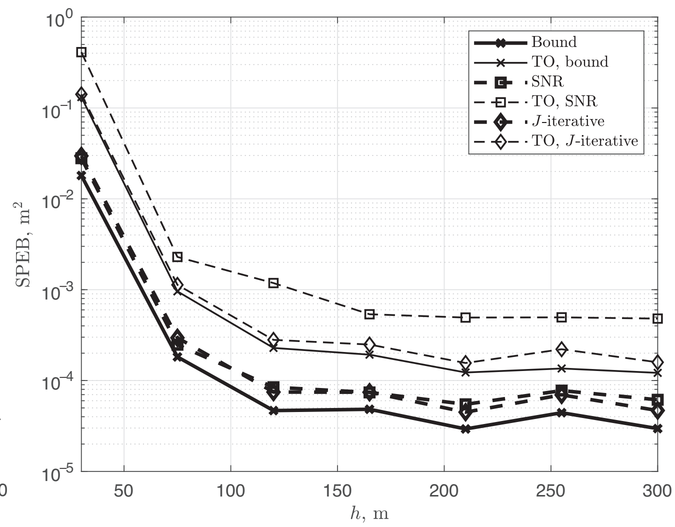

Fig. 4. Impact of the absence of timing synchronization (TO) on the SPEB (bound) using the SNR and J-iterative strategies, as a function of altitude h. For the selection strategies (excluding the bounds), the maximum anchor reduction $N_{R,MAX}$ = 21 is applied.

as a function of the following variables and algorithm options. For each altitude (from 30 to 300 m in steps of 10 m), 200 points are randomly generated on the corresponding horizontal plane, according to a 2D uniform distribution within the area of interest. For each of these points, 50 independent static channel realizations are simulated, leading to a total of 10 000 simulations for each different altitude.

Before presenting and discussing the results, it is worth highlighting that both SPE and SPEB depend on the UAV's position, due to the geometric dilution of precision (GDoP). Particularly, since the altitude estimate error is dominant, accuracy improves when the UAV is located directly above one of the anchors. We observed that the difference in positioning accuracy between the best and worst points is approximately 5 dB. Given that this fluctuation is relatively small, the graphs will present only the average results over different UAV positions within the area of interest, which we believe are reasonably representative of the entire region.

The plots are presented as a function of the

- UAV altitude h, ranging from 30 to 300 m;
- Number of reduced anchors N_R, ranging from 0 (the position is determined exploiting all the available anchors) to the maximum $N_{R,MAX} = N_A - 4$, (N_A denotes the total number of anchors, equal to 25), since at least four anchors are necessary to obtain the 3D position.

The algorithm options that are used for evaluating the multipath impact on performance are:

- NLoS detection, "absent" or "ideal." While in the SPEB computation the NLoS links are always excluded from the theoretical bound, as they do not contribute to the position estimate, in the application of the real algorithm (NLLS), we distinguish between the absence of a specific detection strategy for the NLoS condition and the correct detection and exclusion of all the links that are NLoS. The results in the figures refer to the ideal detection of NLoS conditions and exclusion of the corresponding measures, unless otherwise stated.
- The presence or not of a TO between the set of anchors, which are synchronized, and the UAV. This corresponds to the two cases of algorithms based on ToAs or TDoAs. The quality of the numerical results does not change with or without the TO, i.e., with ToAs or TDoAs, but the absolute values of the SPEB and SPE are decreased.

In Figs 3–5, we can observe how the SPEB and SPE, for the NLLS, change with altitude, without and with the application (down to the minimum number of necessary anchors) of the two main reduction strategies, SNR and J-iterative. The curves are reported with no anchor reduction and with the maximum number of reduced anchors, $N_{R,MAX}$. In addition to the difference between the bound and the real algorithm (NLLS), we can observe the following main aspects, generally confirmed also by the results reported in the sequel:

- The SPE and SPEB decrease with altitude h, at least up to the altitudes of interest for the UAV application, even though the distance between the UAV and the anchors – and, consequently, the path loss – increases. This is due to the dominant improvement of propagation conditions, as the multipath impact and the number of NLoS links decrease with increasing altitude.
- The performance difference between applying or not applying the selection strategies with the maximum anchor reduction is confined within a factor of 10. This confirms that, in the presence of many anchors, it is possible to considerably reduce the number of signals exploited in the estimation process. This reduction has a positive impact on the computational complexity of positioning algorithms and on latency when the device collects distance measures from the anchors serially (downlink positioning).

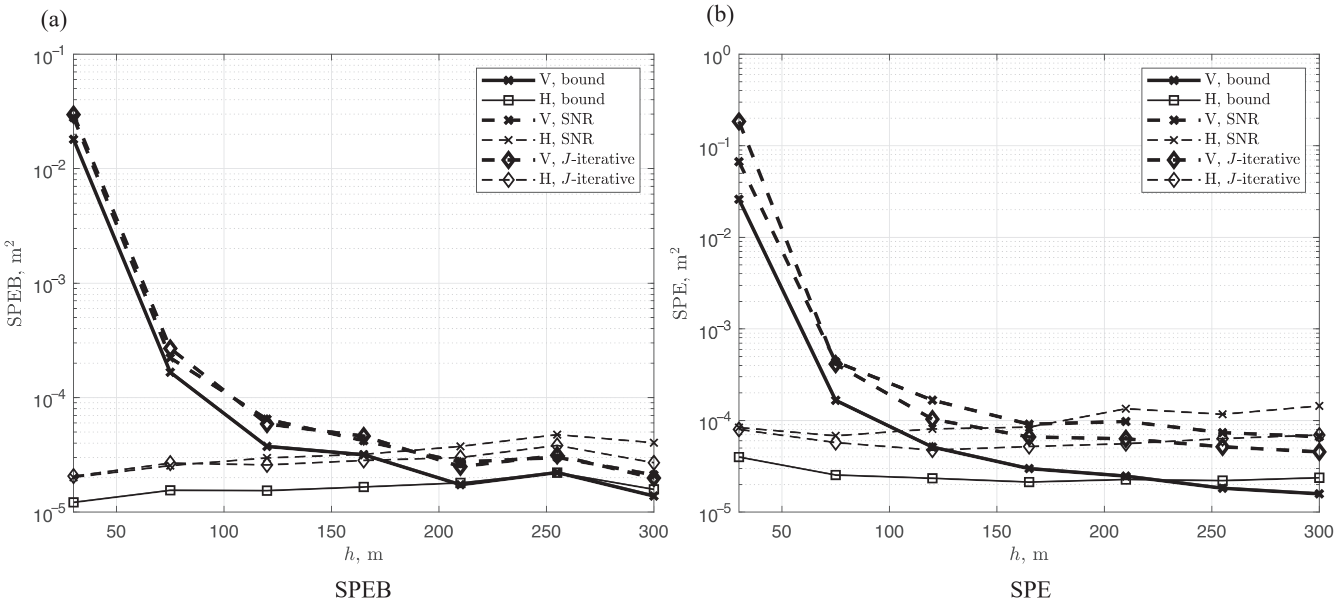

Fig. 5. SPEB (bound) and SPE (NLLS algorithm) with SNR and J-iterative strategies, as a function of the altitude h and separated into their vertical and horizontal components. Except for the bounds, the maximum anchor reduction $N_{R,MAX}$ = 21 is applied.

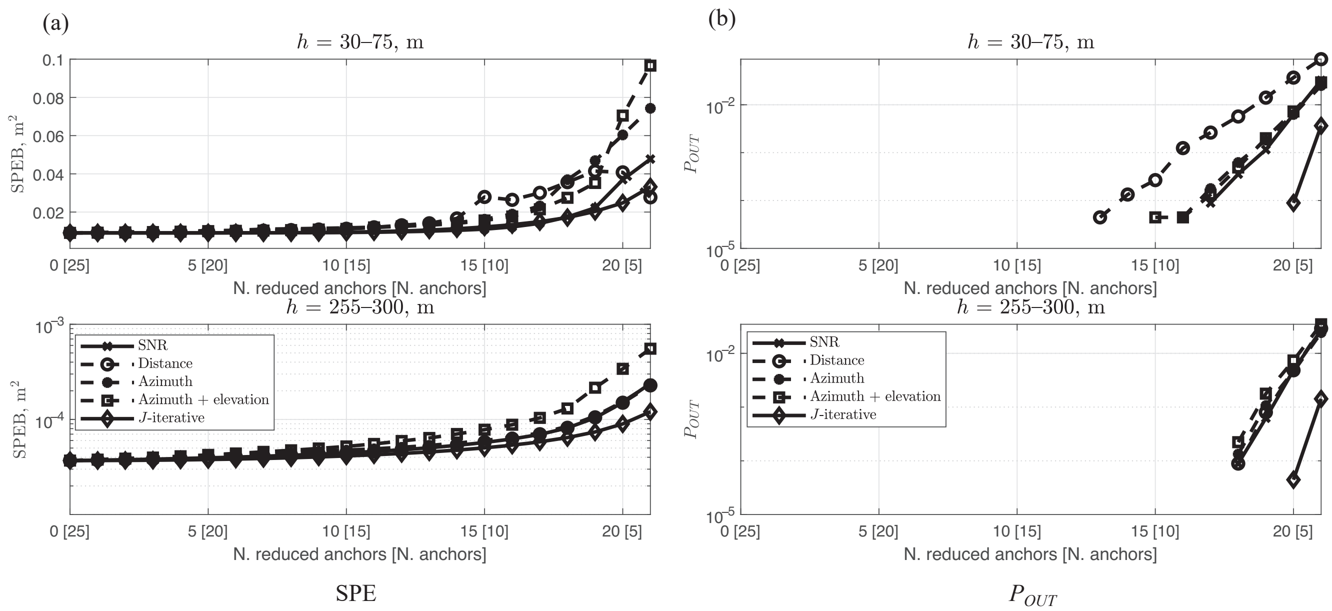

Fig. 6. SPEB (bound) and P_{OUT} as a function of N_R at the two extreme altitude intervals with prior time synchronization (without TO).

- The performance difference between the most complex, J-iterative, and the simplest, SNR-based strategies is also generally low, but becomes more significant when the additional TO needs to be estimated, i.e., in absence of synchronization (Fig. 4).
- It is interesting to notice that the vertical and horizontal components behave differently as a function of the altitude h, both for the SPEB and the SPE: the horizontal component is almost constant, slightly increasing due to the decrease in SNRs, while the vertical component is considerably higher at low h and then decreases rapidly. This is because the increase in relative elevation angles improves the estimation of the vertical component (Fig. 5).

Now Figs 6 and 7 are used as a performance benchmark, as they represent the SPEB as a function of the number of reduced anchors N_R for the different strategies, with and without TO. The results in Figs 6 and 7 – and in the following ones – are obtained by averaging the SPEB or SPE at the two extreme intervals of the altitude range, in order to highlight the performance differences. In fact, comparisons among the different techniques at intermediate altitudes do not provide additional information. We can observe that:

- The main differences among the strategies become more evident at the extreme values of N_R, where some strategies produce higher errors and outliers, as reflected in P_{OUT}. This means that anchor exclusion can result in a geometric layout of the remaining anchors that is no longer compatible with a reliable position estimate.

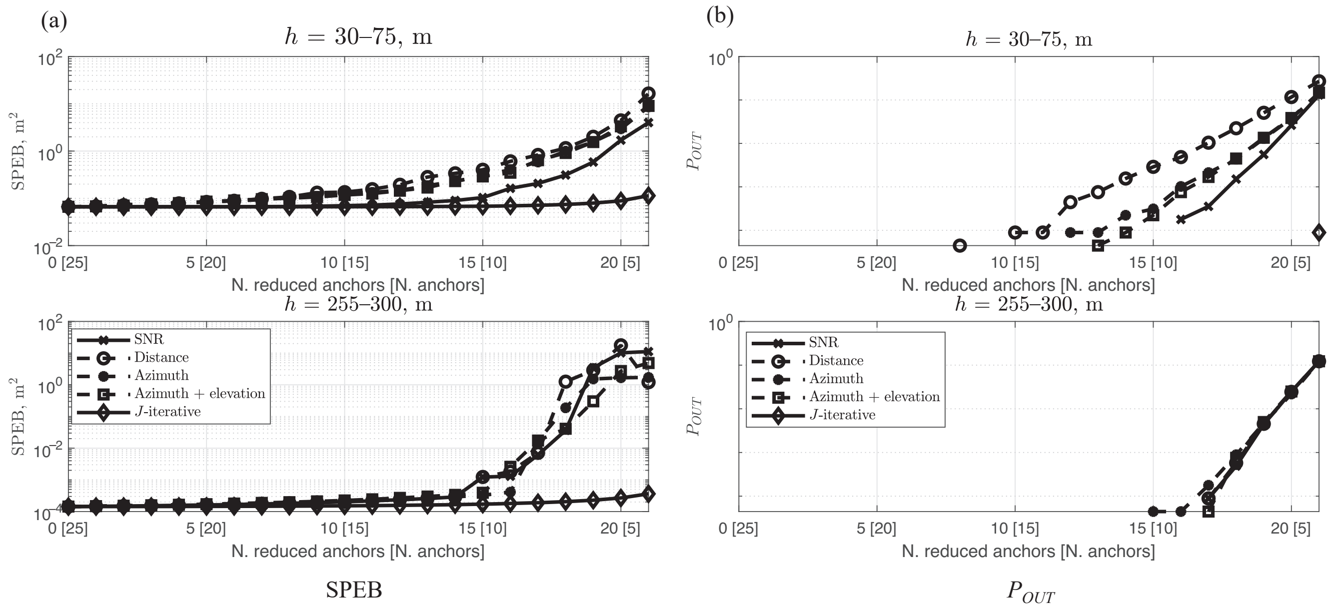

Fig. 7. SPEB (bound) and P_{OUT} as a function of N_R at the two extreme altitude intervals without prior time synchronization.

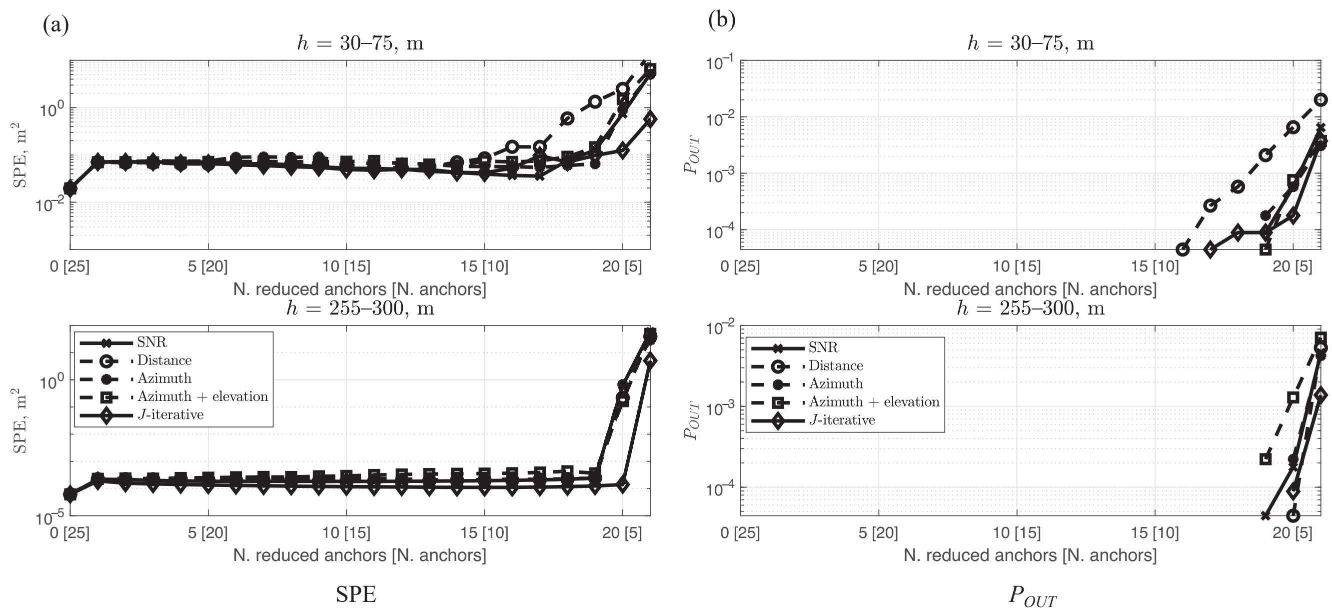

Fig. 8. SPE (NLLS) and P_{OUT} as a function of N_R at the two extreme altitude intervals with prior time synchronization and ideal NLoS detection.

- After the *J*-iterative, which is the best, the SNR-based strategy seems a valid alternative, if the issue related to the presence of outliers at a low number of anchors (high N_R) is managed correctly. The advantage provided by the *J*-iterative is higher in the absence of synchronization, as shown in Fig. 7.
- Between the presence or absence of the TO, there is approximately a performance loss between $10^{0.75}$ and 10, at least for the best strategy. For the other strategies, we observe a remarkable degradation for high values of anchor reduction. This is also confirmed for the NLLS.
- The scenario with the UMa channel model loses approximately a factor of $10^{2.5}$ in the SPEB compared to free space (not reported here). This is also confirmed for the NLLS.

Moving to the application of real algorithms, we can observe and confirm some interesting differences: in Fig. 8, it is clear how the performance does not change significantly with N_R, except in the region close to the maximum anchor reduction, when the geometric outliers produce their impact. At the same time, the SPE tends to decrease with N_R, especially at the beginning of the application of reduction strategies (low N_R); in addition, the loss with respect to the SPEB is within a factor of $10^{0.5}$, and the pure impact of multipath (deactivation of multipath in the channel model) is around $10^{2.5}$ (not shown in the figures). Then, if we add the

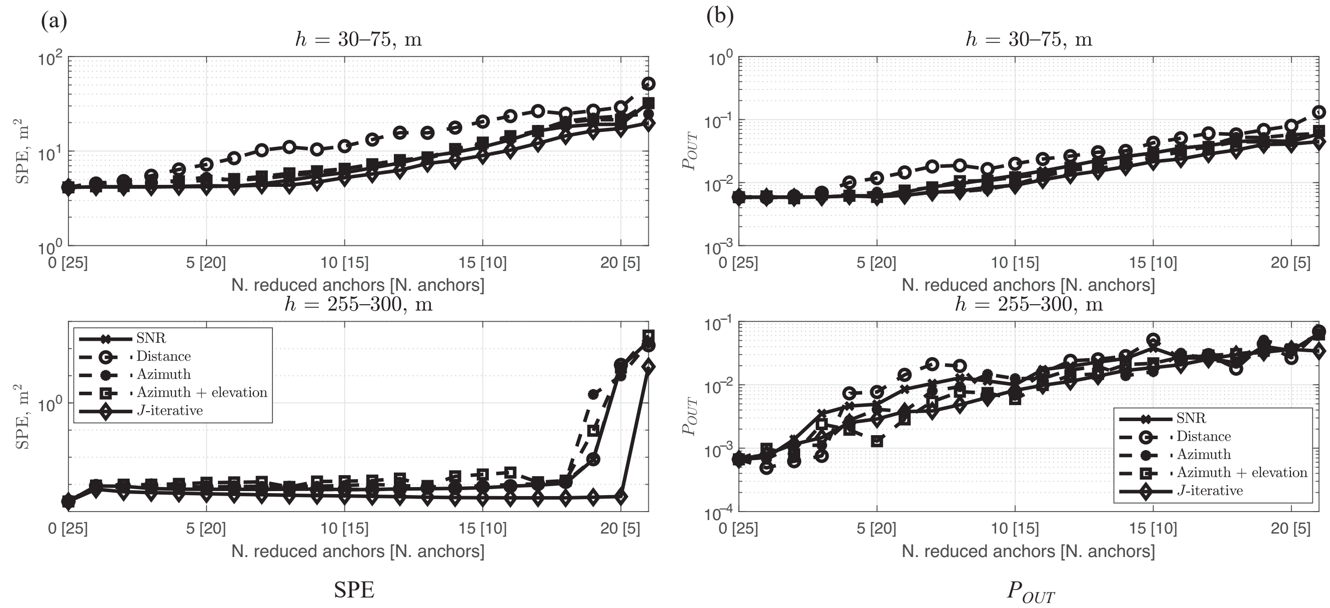

Fig. 9. SPE (NLLS) and P_{OUT} as a function of N_R at the two extreme altitude intervals with ideal NLoS detection and no prior time synchronization (TO).

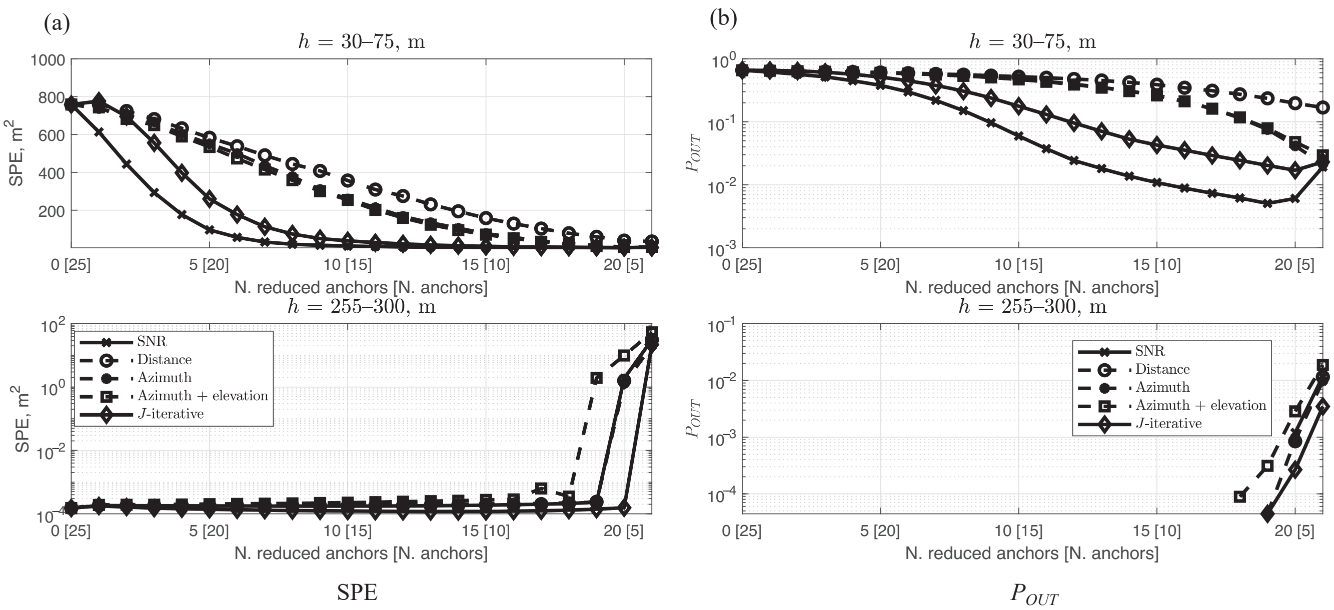

Fig. 10. SPE (NLLS) and P_{OUT} as a function of N_R at the two extreme altitude intervals with prior time synchronization and no NLoS detection.

effect of TO, in Fig. 9, we observe a general performance loss of about $10^{0.5}$ and a reduced difference among the strategies, especially at low altitudes. It is also interesting to notice that, if we deactivate the NLoS detection, we typically observe (i) a general performance decrease, higher at low altitudes, as expected, and (ii) a faster SPE improvement at low-to-medium altitudes as N_R increases, due to the gain obtained by excluding measures that are likely generated by NLoS links. Furthermore, the SNR-based strategy appears to be the best one for this reason at low altitudes, as the SNR is a coarse but valid parameter for distinguishing LoS from NLoS measures. Fig. 10 shows an example of this case.

Finally, Fig. 11 presents the cumulative distribution function (CDF) of the SPEBs with and without TO, in which some of the properties and results already discussed can be observed in more detail: in particular, we can appreciate the advantage provided by the J-iterative strategy in the absence of time synchronization and the impact of outliers, which is included in the CDFs, as they do not achieve the value 1 within the shown error range.

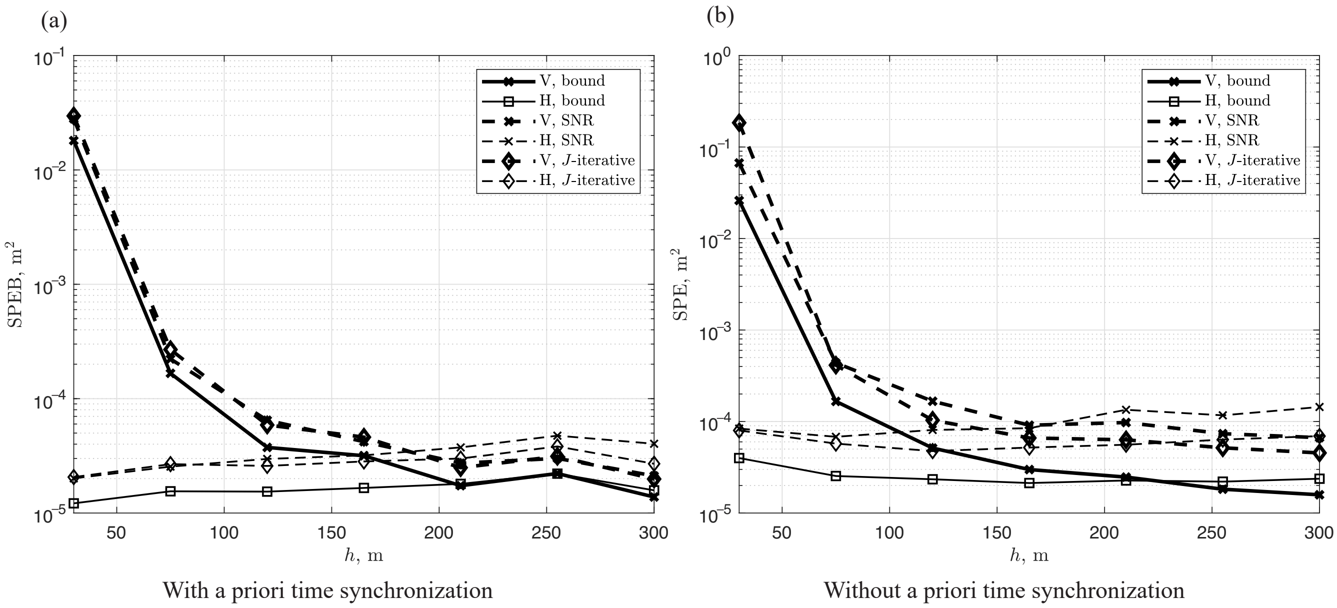

Fig. 11. CDF of SPEB at the two extreme altitude intervals (bold lines refer to h = 30–75 m, and the others to h = 255–300 m) with and without prior time synchronization.

6. Conclusion

This paper focused on the investigation of anchor selection strategies in the context of unmanned aerial vehicle localization in advanced mobile networks, using time-of-arrival- or time-difference-of-arrival-based techniques. We addressed the problem of reducing the number of anchors from a set of available ones, employing different types of information at the UAV in propagation conditions that include realistic path loss, shadowing, and multipath, and applying a least squares-based algorithm in addition to the Cramér–Rao lower bounds. We showed that the number of anchors can be significantly reduced without compromising performance, and that and the corresponding reduction in complexity and latency can also be obtained through simple signal-to-noise-ratio-based techniques, especially at low altitudes. In more challenging conditions, such as the absence of synchronization and anchor reduction close to the maximum, the J-iterative technique demonstrated a clear advantage. In future work, the anchor selection strategies developed here could be further explored through experimental tests, to better evaluate localization accuracy and performance loss due to anchor reduction, while also investigating two-way ranging techniques to synchronize the user equipment with the anchors.

Data availability statement

All data are available in the article.

Acknowledgments

The authors would like to thank Leonardo S.p.A. for funding Alberto Facheris PhD in Information Technology at the Technical University of Milan, as well as the fruitful cooperation that inspired the topic covered in this article. The publication costs of this article were partially covered by the Estonian Academy of Sciences.

References

3GPP. 2017. *Technical Specification Group Radio Access Network: Study on Enhanced LTE Support for Aerial Vehicles (Release 15), v. 15.0.0*. TR 36.777.

3GPP. 2018a. *Release 15 Specifications*. https://www.3gpp.org/specifications-technologies/releases/release-15

3GPP. 2018b. *Technical Specification Group Services and System Aspects: Study on Positioning Use Cases – Stage 1 (Release 16), v. 16.1.0*. TR 22.872.

3GPP. 2019. *Technical Specification Group Services and System Aspects: Enhancement for Unmanned Aerial Vehicles – Stage 1 (Release 17), v. 17.1.0*. TR 22.829.

3GPP. 2021. *Technical Specification Group Services and System Aspects: Study on Supporting Unmanned Aerial Systems (UAS) Connectivity, Identification and Tracking (Release 17), v. 17.1.0*. TR 23.754.

3GPP. 2022. *Release 17 Specifications*. https://www.3gpp.org/specifications-technologies/releases/release-17

3GPP. 2023a. *Release 18 Specifications*. https://www.3gpp.org/specifications-technologies/releases/release-18

3GPP. 2023b. *Technical Specification Group Radio Access Network: Solutions for NR to Support Non-Terrestrial Networks (NTN) (Release 16), v. 16.2.0*. TR 38.821.

3GPP. 2023c. *Technical Specification Group Services and System Aspects: Release 17 Description – Summary of Rel-17 Work Items (Release 17), v. 17.0.1*. TR 21.917.

Albaidhani, A., Morell, A. and Vicario, J. L. 2019. Anchor selection for UWB indoor positioning. *Trans. Emerg. Telecommun. Technol.*, **30**(6). https://doi.org/10.1002/ett.3598

Bar-Shalom, Y., Li, X.-R. and Kirubarajan, T. 2002. Linear estimation in static systems. In *Estimation with Applications to Tracking and Navigation: Theory, Algorithms and Software*. John Wiley and Sons, 121–177. https://doi.org/10.1002/0471221279.ch3

Deng, Z., Wang, H., Zheng, X. and Yin, L. 2020. Base station selection for hybrid TDOA/RTT/DOA positioning in mixed LoS/NLoS environment. *Sensors*, **20**(15), 4132. https://doi.org/10.3390/s20154132

Facheris, A. and Reggiani, L. 2023. SPEB evaluation and anchors selection for UAV positioning. In *European Wireless 2023; 28th*

European Wireless Conference, Rome, Italy, 2–4 October 2023. IEEE, 2024, 124–129.

Reggiani, L. and Facheris, A. 2024. Impact of multipath on anchors selection strategies for UAVs positioning in mobile networks. In *2024 19th Biennial Baltic Electronics Conference (BEC), Tallinn, Estonia, 2–4 October 2024*. IEEE, 2024, 1–6. https://doi.org/10.1109/BEC61458.2024.10737946

Shen, Y. and Win, M. Z. 2010. Fundamental limits of wideband localization – Part I: a general framework. *IEEE Trans. Inf. Theory*, **56**(10), 4956–4980. https://doi.org/10.1109/TIT.2010.20 60110

Wang, D., Fattouche, M. and Ghannouchi, F. M. 2017. Bounds of mmWave-based ranging and positioning in multipath channels. In *2017 IEEE Globecom Workshops (GC Wkshps), Singapore, 4–8 December 2017*. IEEE, 2018, 1–6. https://doi.org/10.1109/GLOCOMW.2017.8269035

Xhafa, A., del Peral-Rosado, J. A., López-Salcedo, J. A. and Seco-Granados, G. 2022. Evaluation of 5G positioning performance based on UTDoA, AoA and base-station selective exclusion. *Sensors*, **22**(1), 101. https://doi.org/10.3390/s22010101

Mitmerajalisuse mõju ankrute valikustrateegiatele droonide lokaliseerimisel mobiilsidevõrkudes

Luca Reggiani ja Alberto Facheris

Artikkel käsitleb ankrute valikustrateegiaid droonide (UAV) lokaliseerimiseks mobiilsidevõrkudes, kasutades signaali saabumisajal (ToA) ja signaali saabumisaegade erinevusel (DToA) põhinevaid tehnikaid. Uurisime, kuidas vähendada ankrute arvu ilma täpsust kaotamata, arvestades realistlikke levitingimusi, nagu tee kadu, varjutus ja mitmerajalisus. Rakendades vähimruutude algoritmi ja Cramér–Rao alumisi piire (CRLB), näitavad tulemused, et ankrute arvu saab oluliselt kahandada ilma sooritust ohustamata ning et keerukust ja latentsust saab vähendada ka lihtsate signaali-müra suhtel põhinevate tehnikate abil, eriti madalatel kõrgustel. Raskemates tingimustes, näiteks sünkroonimata süsteemides või ankrute maksimaalse vähendamise korral, osutub *J*-iteratiivne meetod tõhusaimaks. Edasised uuringud võiksid hõlmata eksperimentaalseid katseid, et veelgi paremini hinnata lokaliseerimistäpsust ja ankrute vähendamise mõju.